

# Investigation of the Hydrogen-Bonding Structure and Miscibility for PU/EP IPN Nanocomposites by PALS

Yuchan Zhu,<sup>†</sup> Bo Wang,<sup>\*,†</sup> Wei Gong,<sup>†</sup> Lingmei Kong,<sup>†</sup> and Qingming Jia<sup>‡</sup>

Department of Physics, Wuhan University, Wuhan 430072, China, and School of Material Science and Technology, Xi'an Jiaotong University, Xi'an 710049, China

Received September 10, 2006; Revised Manuscript Received November 3, 2006

**ABSTRACT:** Effects of hydrogen bonding on the free volume and miscibility were first investigated for polyurethane/epoxy resin (PU/EP) interpenetrating polymer network (IPN) nanocomposites by positron annihilation lifetime spectroscopy (PALS), Fourier transform infrared spectroscopy (FTIR), and dynamic mechanical analysis (DMA). Infrared spectroscopy suggested that the strengths of two kinds of hydrogen-bonding interactions including both between carbonyl group and N–H group and the other between urethane group in PU and silicate layers depended strongly on the dispersed state of the layered montmorillonite (MMT) in the matrix. We found that the stronger the hydrogen-bonding interaction, the higher the average chain packing efficiency and the smaller the free volume hole size, the better the miscibility. On the other hand, from the analyses of distributions of the free volume and the loss factor, it is very interesting that the large differences between the exfoliated structure and the intercalated structure of MMT were observed.

## Introduction

In recent years, the polymer-layered silicate (PLS) nanocomposites have attracted considerable attention because of their unique properties such as increased modulus, improved gas permeability, and thermal stability.<sup>1,2</sup> It is well-known that the dispersion state of the clays and the polymer–clay interaction are of great significance for the design of tailored polymer systems with enhanced properties because these factors play an important role in determining the physical and chemical properties. Large amounts of work have already been done on MMT-filled nanocomposites.<sup>3–5</sup>

Recently, interpenetrating polymer network (IPN) has been paid more attention and studied extensively.<sup>6,7</sup> IPN is one kind of polymer alloy consisting of two or more distinct cross-linked polymer networks held together by permanent entanglement and shows excellent engineering properties due to a synergetic effect induced by the forced compatibility of the individual components.<sup>8</sup> Most IPN show phase separation, and a lot of work has already been done on the improvement of miscibility of IPN.<sup>9</sup> However, little information concerning MMT-filled IPN and its microstructure has been investigated. A better understanding of the microstructure in nanocomposite is very important for molecular insight and leads to the design of nanocompositional materials with improved properties. Some research work indicated that the hydrogen bond plays an important role in determining the free volume and the miscibility of polymer blends.<sup>10</sup> Previous work has shown that increasing the strength of hydrogen-bonding interactions in polymer blends produces changes in the network structure.<sup>11</sup> The investigation of effects of hydrogen-bonding interactions on the microstructure and the miscibility is very important for MMT-filled IPN.

Positron annihilation lifetime spectroscopy (PALS) has been become an increasing important method to detect atomic-scale microstructure in polymers currently.<sup>12–14</sup> Positron probe is a sensitive tool to detect nanohole volumes and has been widely

used to study the microstructure of polymers. It is based on the fact that the lifetimes of positron and its bound forms (positronium: Ps, bound state of  $e^+$  and  $e^-$ ) are sensitive to the existence of structural inhomogeneities because the formation and annihilation of Ps are localized in nano- or subnanoscale level holes.<sup>15–18</sup> An orthopositronium (o-Ps: the triple bound state of Ps) probe has a relatively small diameter (0.106 nm) and a repulsive nature compared with the atoms and molecules in a substance; thus one can obtain information about defect, atomic vacancy, and free volume. In this work, the PALS, XRD, DMA, and FTIR were first employed to study the effect of hydrogen-bonding interactions on the free volume and miscibility for the PU/EP IPN nanocomposites.

## Experimental Part

**Materials and Sample Preparation.** The commercial 2,4-toluene diisocyanate (TDI) and octadecylammonium chloride were supplied by Shanghai Chemical Reagent Co. (China). Commercial castor oil, diglycidyl ether of biphenol A (DGEBA), and 2,4,6-tri-(dimethylaminomethyl)phenol (DMP-30) were made in Tianjin Chemical Co. (China). The sodium montmorillonite with a cation exchange capacity (CEC) of 90–100 mmol/100 g was provided by South Clay Co. (China). The MMT is organically modified by a hexadecylammonium ion to enhance compatibility with matrix. Castor oil and DGEBA were dried under vacuum prior to use. Castor oil and 0, 1, 3, and 5 wt % of org-MMT were placed in a round-bottomed flask, heated, and stirred for about 4 h. Quantitative TDI was added after the system cooled down. Then the blends were stirred again under a dry nitrogen atmosphere for about 45 min to form urethane prepolymer. The appropriate weights of the epoxy precursor and DMP-30 were successively added to the system. The mixture was degassed under vacuum for several minutes and cured at 120 °C in the preheated Teflon molds for several hours. IPN/MMT0, IPN/MMT1, IPN/MMT3, and IPN/MMT5 are named to denote the nanocomposites with 0, 1, 3, and 5 wt % MMT, respectively. Details of the samples can be found in the previous work.<sup>19</sup>

**Experimental Method.** All PAL spectra were recorded at room temperature using a fast–fast coincidence system with a time resolution of about 270 ps. A 20  $\mu$ Ci  $^{22}\text{Na}$  positron source was sandwiched between two pieces of the same samples. Each spectrum contained approximately 1 million and 4 million counts for

<sup>†</sup> Wuhan University.

<sup>‡</sup> Xi'an Jiaotong University.

\* Corresponding author: Tel +86-27-68753880; fax +86-27-87654569, e-mail bwang@positron.whu.edu.cn.

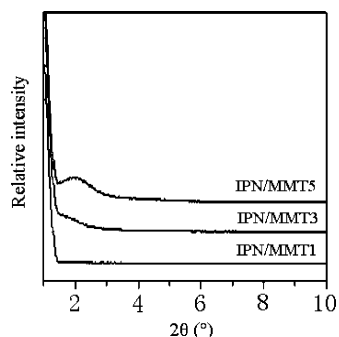


**Figure 1.** X-ray diffraction curves of IPN/MMT1, IPN/MMT3, and IPN/MMT5.

PATFIT<sup>20</sup> and MELT,<sup>21–24</sup> respectively. All the measured spectra were resolved into three components using PATFIT for discrete analysis. The first lifetime component  $\tau_1$  ( $\sim 125$  ps) and the second lifetime component  $\tau_2$  ( $\tau_2 = 300$ – $350$  ps) are attributed to the self-annihilation of parapositronium (p-Ps) and the positron annihilation, respectively. The third lifetime component  $\tau_3$  ( $\tau_3 = 1.4$ – $2.6$  ns) results from the pick-off annihilation of o-Ps in the free volume holes. There is a relation between o-Ps lifetime and radius of the free volume hole as follows:<sup>25</sup>

$$\tau_3 = \frac{1}{2} \left[ 1 - \frac{R}{R + \Delta R} + \frac{1}{2\pi} \sin\left(\frac{2\pi R}{R + \Delta R}\right) \right]^{-1} \quad (1)$$

where  $R$  is the radius of the free volume hole;  $\Delta R = 1.656 \text{ \AA}$ <sup>26</sup> derived from fitting the observed o-Ps lifetimes in molecular solids with known hole sizes. The average free volume size was calculated using

$$V = \frac{4\pi R^3}{3} \quad (2)$$

X-ray diffraction (XRD) experiments were performed at room temperature using a Rigaku D/max-2400 diffractometer with Cu K $\alpha$  radiation ( $\lambda = 0.15418 \text{ nm}$ ). The samples were placed inside the sample holder at the rate  $2 \text{ }^\circ\text{C/min}$ . The microscale dispersion of different content of MMT in nanocomposites was determined using an H-600 transmission electron microscope (Hitachi Co., Japan). The Fourier transform infrared spectra were used to determine the strength of the hydrogen-bonding using an IRrestige-21 FT-IR (Shimadzu, Japan). The loss factor ( $\tan \delta$ ) was determined using the DMA Q800 equipment (TA Co.) in the temperature range from  $-40$  to  $40 \text{ }^\circ\text{C}$  at  $1 \text{ Hz}$  at heating  $3 \text{ }^\circ\text{C/min}$  and the three-point bending mode under a dry nitrogen atmosphere.

## Results and Discussion

XRD curves for all the nanocomposites are shown in Figure 1. According to Bragg's law, the spacing of the MMT layers in nanocomposites can be determined from the angle of diffraction peak using the relation as follows:

$$2d \sin \theta = n\lambda \quad (3)$$

From Figure 1, the diffraction peak is clearly observed in the curve of IPN/MMT5, which indicates that an intercalated structure has been formed, while this diffraction peak does not appear in the IPN/MMT1 and IPN/MMT3. However, there is an evident difference between the curves of IPN/MMT1 and IPN/MMT3; i.e., the curve of IPN/MMT3 has a broad peak in the small angle region, which means that the MMT platelets are not completely exfoliated in IPN/MMT3. So the information obtained from XRD curve shows that the exfoliation degree of MMT platelets in IPN matrix at low MMT concentration (1 wt %) is higher than that at high MMT contents (3 and 5 wt %), which has been confirmed by TEM measurement as shown in

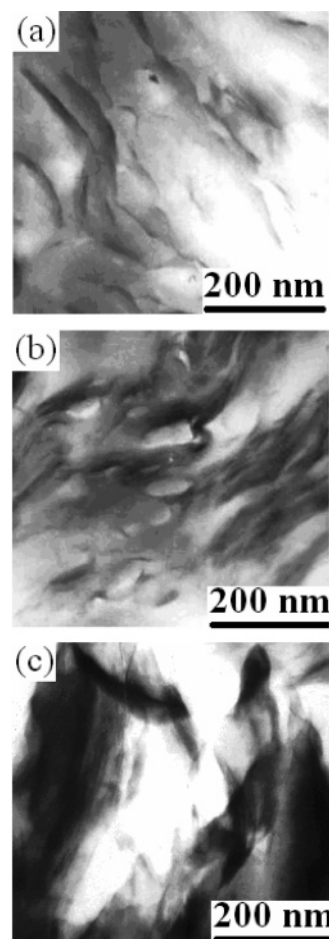


**Figure 2.** TEM micrographs for (a) IPN/MMT1, (b) IPN/MMT3, and (c) IPN/MMT5.

Figure 2. TEM micrographs are illustrated in parts a, b, and c of Figure 2 for IPN/MMT1, IPN/MMT3, and IPN/MMT5, respectively. The dark areas are the intersections of MMT layers dispersed in the matrix. It can be seen that the MMT platelets are mostly exfoliated and dispersed homogeneously in the IPN/MMT1, whereas IPN/MMT3 is typically mixed structure of intercalated and exfoliated nanoclay morphology. In Figure 2c, we found that the agglomeration of the MMT layers occurred in matrix. XRD results, together with TEM observation, indicate that low content (1 wt %) of the MMT can be more easily exfoliated compared with that of higher contents (3 and 5 wt %). The differently dispersed states of MMT have an important effect on the microstructure.

**Effect of Hydrogen Bonding on Free Volume.** The lifetime of o-Ps,  $\tau_3$ , as a function of weight percent of org-MMT in nanocomposites is shown in Figure 3. According to eq 1,  $\tau_3$  is correlated with the size of the free volume holes. The average free volume size is calculated using eqs 1 and 2 in a spherical-hole model and is shown on the right vertical axis. In Figure 3, we found that  $\tau_3$  decreases evidently when MMT is added, and the variation of the free volume hole size is similar to the  $\tau_3$ ; i.e., the free volume holes decrease after loaded MMT, indicating the nanocomposites have a higher chain packing efficiency compared to PU/EP IPN unloaded MMT. Maybe the decrease in size of free volume hole in IPN/MMT results from the conformational changes to polymer molecules<sup>27</sup> due to the constrained interaction (such as hydrogen-bonding interaction between carbonyl group and N–H group). The hydrogen-bonding interaction was studied by Fourier transform infrared spectra as shown in Table 1 for IPN/MMT0, IPN/MMT1, IPN/

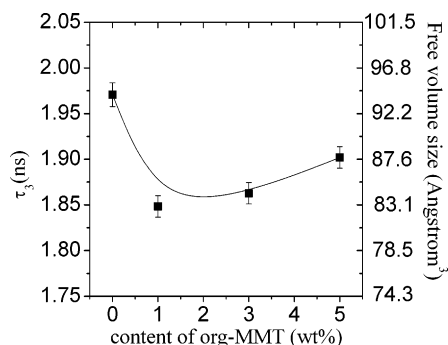


**Figure 3.** Lifetime of o-Ps,  $\tau_3$ , as a function of weight percent of org-MMT, and the average free volume size is shown on the right vertical axis. The line is drawn to guide the eye.

**Table 1**

samples	carbonyl ( $\text{cm}^{-1}$ )		H-bonding index ( $R$ )
	bonded carbonyl	free carbonyl	
IPN/MMT0	1710	1740	0.812
IPN/MMT1	1710	1740	0.870
IPN/MMT3	1710	1740	0.961
IPN/MMT5	1710	1740	0.885

MMT3, and IPN/MMT5. The carbonyl ( $\text{C}=\text{O}$ ) absorption peak is split distinctly into two peaks in all samples: one is at  $1740\text{ cm}^{-1}$  and the other is at  $1710\text{ cm}^{-1}$ . These can be attributed to free and bonded carbonyl of urethane group, respectively.<sup>28</sup> The observed ratio  $\Delta\nu/\nu$  of 0.017 for the carbonyl splitting is in agreement with values published for hydrogen-bonded  $\text{C}=\text{O}$  groups in other compounds.<sup>29</sup> So we can conclude that the hydrogen bonding has formed between the carbonyl group and N—H group in all samples, which agrees with earlier studies about hydrogen-bonding interaction between carbonyl group and N—H group in PU.<sup>28,30</sup> In addition, the relative absorbances of the two carbonyl peaks should serve as an index of the degree to which this group participates in hydrogen bonding.<sup>28</sup> The hydrogen bonding index  $R$  may be defined as the ratio of the absorbances  $A_{1710}/A_{1740}$ ; greater values of  $R$  indicate increased participation of the carbonyl group in hydrogen bonding.<sup>28</sup> From Table 1, it is clear that the nanocomposites has higher degree of hydrogen bonding compared with the IPN unloaded MMT, which means that the addition of MMT improves the formation of hydrogen bonding. According to the reports by Etxeberria and Rao et al.,<sup>31,32</sup> hydrogen bonding can improve the cross-linking density of materials, which brings about a higher chain packing efficiency. Compact arrangement of molecular chains leads to the decrease of average free volume size in nanocomposites. This is consistent with the report by Cowie et al.;<sup>10</sup> i.e., the enhancement of the hydrogen-bonding brings about a decrease of the free volume.

On the other hand, from the variation of the free volume hole as a function of the MMT content, we found that the sample of 1 wt % MMT content has the smallest free volume size; then, the size of the free volume hole increases slightly with increasing the content of MMT, which indicates that the chain packing efficiency gradually decreases. It can be explained by the interfacial interaction between the MMT and matrix. In IPN/MMT nanocomposites, there are two kinds of hydrogen bonding interaction: one is formed between carbonyl group and N—H group (as mentioned above), and the other is formed between urethane group in PU and silicate layers as shown in Figure 4. This formation of the hydrogen bonding between the surface of MMT platelets and urethane of PU can be found in earlier studies.<sup>33–35</sup> In mostly exfoliated state, a bigger surface area of

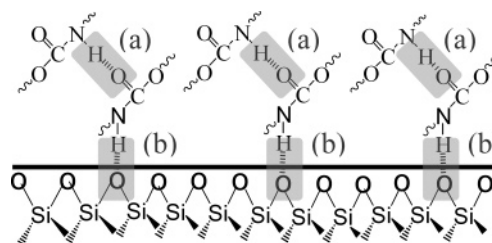


**Figure 4.** Schematic of formation of hydrogen bonds: (a) is formed between carbonyl group and N—H group, and (b) is formed between urethane group in PU and silicate layers.

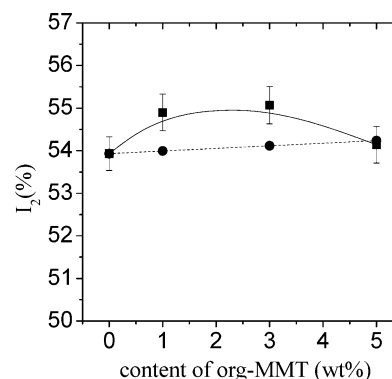


**Figure 5.** Second lifetime intensity  $I_2$  vs the org-MMT content. The experiment data are denoted by squares, and the data of G. Consolati et al. and S. J. Wang et al. are represented as circles.

dispersed phase is benefit to the formation of hydrogen bonding as shown in Figure 4, which makes it easier for the polymer chains to pack more closely. However, in intercalated and agglomerated state, the poor interaction between stacked MMT and PU/EP matrix has little restriction on the segmental mobility due to less contacting area between the MMT and the matrix,<sup>3</sup> which leads to less formation of hydrogen bonding between urethane group in PU and silicate layers. This result shows that the dispersed degree of MMT within polymer matrix plays a vital role in determining the microstructure.<sup>36</sup>

In order to further study the influence of the content of MMT on the microstructure, the variation of the second lifetime intensity  $I_2$  as a function of the MMT content has been discussed as shown in Figure 5. According to the reports,<sup>37,38</sup> the variation of  $I_2$  is related to the interfacial interaction in the nanocomposites. Supposing there is no interfacial interaction between MMT and matrix, according to the simple mixture rule, it only comes from positron annihilation in MMT and matrix,  $I_2$  should be linearly additive basis on the weight fraction,<sup>37</sup> and we have

$$I_2^N = I_2^M \Phi_w + I_2^I (1 - \Phi_w) \quad (4)$$

where the superscripts M, I, and N refer to the MMT, PU/EP IPNS, and nanocomposites, respectively. In terms of the values reported by Consolati and Wang,<sup>38,39</sup> the second lifetime can be calculated approximately the  $I_2^N$  as shown in Figure 5. It is obvious that the experimental data show a positive deviation in IPN/MMT1 and IPN/MMT3, which indicates that the interfacial interaction between MMT platelets and matrix exists. Wang et al.<sup>3</sup> discovered that strong interfacial interaction caused an apparent reduction in the average free volume size. In addition, lower value of  $I_2$  for IPN/MMT5 was observed, which agrees with the less formation of hydrogen bonding between urethane group in PU and silicate layers in IPN/MMT5. This result testifies again that the dispersion of MMT within polymer matrix plays an important role in determining the microstructure.



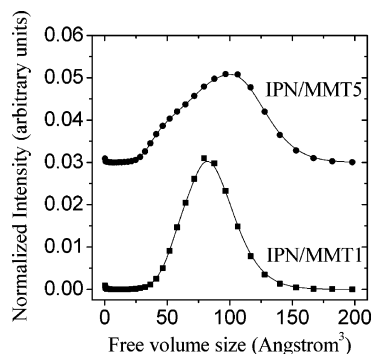


Figure 6. Free volume distribution of IPN/MMT1 and IPN/MMT5.

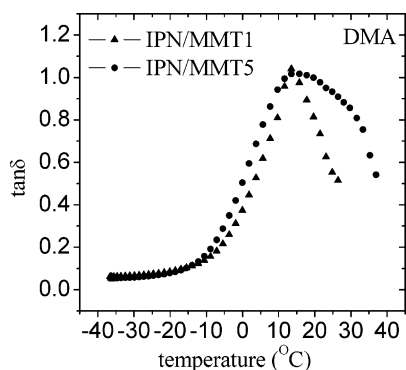


Figure 7. DMA curve of IPN/MMT1 and IPN/MMT5.

**Effect of Hydrogen Bonding on Miscibility.** In order to discuss the effect of hydrogen-bonding interactions on the miscibility of IPN nanocomposites, a MELT program was used to obtain the free volume distribution. Figure 6 shows the free volume distributions for IPN/MMT1 and IPN/MMT5. Qualitatively, the maximum of the distribution shifts to higher value with increasing MMT content; this is good agreement with the discrete analysis as shown in Figure 3. On the other hand, it is very interesting that a large difference between IPN/MMT1 and IPN/MMT5 in the free volume distribution is observed. The distribution of IPN/MMT1 is quite narrow and symmetric but extremely broad and unsymmetric for IPN/MMT5. It is well-known that the free volume distribution should have very similar Gaussian-like distributions in the miscible system, while the distribution is broader and unsymmetrical in the immiscible system.<sup>14,40,41</sup> So the miscibility of IPN/MMT1 is better than that of IPN/MMT5, which indicates that the miscibility is greatly affected by the degree of exfoliated and dispersed MMT and the strength of the hydrogen-bonding interaction. This explanation is consistent with the analysis of  $I_2$ , which has also been confirmed by the DMA result. Figure 7 shows the DMA curves of IPN/MMT1 and IPN/MMT5. It is obvious that the peak of  $\tan \delta$  for IPN/MMT5 is much broader compared to that for IPN/MMT1. A broader peak is observed in the higher temperature region. The width of the transition zone in the DMA curve is usually an indication of miscibility or compatibility.<sup>42,43</sup> As mentioned above, we conclude that the stronger the hydrogen-bonding interaction and the better the miscibility of IPN/MMT.

## Conclusion

The influences of hydrogen-bonding interaction on the free volume and the miscibility for the PU/EP IPN nanocomposites were first investigated by PALS, XRD, FTIR, DMA, and TEM. The experimental results indicate that the higher the exfoliated degree of MMT in matrix, the stronger the hydrogen-bonding interaction between the filler and matrix. Stronger hydrogen-

bonding interaction brings about an increment of segmental packing density and a decrease in free volume size. The experimental results indicate that the better the MMT dispersed, the bigger the contacted area between the MMT and IPN matrix, the stronger the interaction. On the other hand, we found that the distributions of both free volume hole and the loss factor are two sensitive indications for determining the miscibility of IPN/MMTs.

**Acknowledgment.** This work was financially supported by the National Natural Science Foundation of China and the Hubei Key Laboratory of Nuclear Solid State Physics.

## References and Notes

- (1) Becker, O.; Cheng, Y.-B.; Varley, R. J.; Simon, G. P. *Macromolecules* **2003**, *36*, 1616.
- (2) Park, J. H.; Jana, S. C. *Macromolecules* **2003**, *36*, 2758.
- (3) Wang, Y.-Q.; Wu, Y.-P.; Zhang, H.-F.; Zhang, L.-Q.; Wang, B.; Wang, Z.-F. *Macromol. Rapid Commun.* **2004**, *25*, 1973.
- (4) Lincoln, D. M.; Vaia, R. A.; Krishnamoorti, R. *Macromolecules* **2004**, *37*, 4554.
- (5) Lim, S. K.; Kim, J. W.; Chin, I.; Kwon, Y. K.; Choi, H. J. *Chem. Mater.* **2002**, *14*, 1989.
- (6) Huelck, V.; Thomas, D. A.; Sperling, L. H. *Macromolecules* **1972**, *5*, 340.
- (7) Frisch, H. L.; Frisch, K. C.; Klempner, D. *Polym. Eng. Sci.* **1974**, *14*, 646.
- (8) Sperling, L. H. *Interpenetrating Polymer Networks and Related Materials*; Plenum Press: New York, 1981.
- (9) Dueñas, J. M. M.; Escuriola, D. T.; Ferrer, G. G.; et al. *Macromolecules* **2001**, *34*, 5525.
- (10) Cowie, J. M. G.; McEwan, I.; McEwen, I. J.; Pethrich, R. A. *Macromolecules* **2001**, *34*, 7071.
- (11) Cowie, J. M. G.; Reilly, A. A. N. *Polymer* **1992**, *33*, 4814.
- (12) Gong, W.; Mai, Y.; Zhou, Y.; Qi, N.; Wang, B.; Yan, D. *Macromolecules* **2005**, *38*, 9644.
- (13) Wang, B.; Wang, Z. F.; Zhang, M.; Liu, W. H.; Wang, S. J. *Macromolecules* **2002**, *35*, 3993.
- (14) Liu, J.; Jean, Y. C.; Yang, H. *Macromolecules* **1995**, *28*, 5774.
- (15) Brandt, W.; Berko, S.; Walker, W. W. *Phys. Rev.* **1960**, *120*, 1289.
- (16) Shrader, D. M.; Jean, Y. C. *Positron and Positronium Chemistry*; Elsevier: Amsterdam, 1988.
- (17) Wang, C.-L.; Maurer, F. H. J. *Macromolecules* **1996**, *29*, 8249.
- (18) Hristov, H. A.; Bolan, B.; Yee, A. F.; Xie, L.; Gidley, D. W. *Macromolecules* **1996**, *29*, 8507.
- (19) Jia, Q.; Zheng, M.; Chen, H.; Shen, R. *Mater. Lett.* **2006**, *60*, 1306.
- (20) Kirkegaard, P.; Eldrup, M.; Mogensen, O. E.; Pedersen, N. J. *Comput. Phys. Commun.* **1981**, *23*, 307.
- (21) Shukla, A.; Peter, M.; Hoffmann, L. *Nucl. Instrum. Methods A* **1993**, *335*, 310.
- (22) Wästlund, C.; Maurer, F. H. J. *Macromolecules* **1997**, *30*, 5870.
- (23) Dammert, R. M.; Maunu, S. L.; Maurer, F. H. J.; Neelov, I. M.; Niemelä, S.; Sundholm, F.; Wästlund, C. *Macromolecules* **1999**, *32*, 1930.
- (24) Stüvegh, K.; Klapper, M.; Domján, A.; Mullins, S.; Wunderlich, W.; Vértess, A. *Macromolecules* **1999**, *32*, 1147.
- (25) Tao, S. J. *J. Chem. Phys.* **1972**, *56*, 5499.
- (26) Nakanishi, H.; Wang, S. J.; Jean, Y. C. *Positron Annihilation Studies of Fluids*; World Science, Singapore, 1987; p 292.
- (27) Mackay, M. E.; Dao, T. T.; Tuteja, A.; et al. *Nat. Mater.* **2003**, *2*, 762.
- (28) Seymour, R. W.; Estes, G. M.; Cooper, S. L. *Macromolecules* **1970**, *3*, 579.
- (29) Pimentel, G. C.; McClellan, A. L. *The Hydrogen Bond*; W. H. Freeman and Co.: San Francisco, CA, 1960; pp 136–140.
- (30) Coleman, M. M.; Skrovanek, D. J.; Hu, J.; Painter, P. C. *Macromolecules* **1988**, *21*, 59.
- (31) Etxeberria, A.; Guezala, S.; Iruin, J. J.; de la Campa, J. G.; de Abajo, J. *Polymer* **1998**, *39*, 1035.
- (32) Rao, V.; Ashokan, P. V.; Shridhar, M. H. *Polymer* **1999**, *40*, 7167.
- (33) Koo, C. M.; Ham, H. T.; Choi, M. H.; Kim, S. O.; Chung, I. J. *Polymer* **2003**, *44*, 681.
- (34) Francis, C. W. *Soil Sci.* **1973**, *15*, 40.
- (35) Ray, S. S.; Okamoto, M. *Prog. Polym. Sci.* **2003**, *28*, 1539.
- (36) Liu, T.; Lim, K. P.; Tjiu, W. C.; Pramoda, K. P.; Chen, Z.-K. *Polymer* **2003**, *44*, 3529.

- (37) Wang, S. J.; Wang, C. L.; Zhu, X. G.; Qi, Z. N. *Phys. Status Solidi A* **1994**, *142*, 275.
- (38) Wang, S. J.; Zhang, M.; Liu, L. M. *Mater. Sci. Forum* **2004**, *355*, 445–446.
- (39) Consolati, G.; Natali-Sora, I.; Pelosato, R.; Quasso, F. *J. Appl. Phys.* **2002**, *91*, 1928.
- (40) Wästlund, C.; Berndtsson, H.; Maurer, F. H. J. *Macromolecules* **1998**, *31*, 3322.
- (41) Chen, Z. Q.; Uedono, A.; Li, Y. Y.; He, J. S. *Jpn. J. Appl. Phys.* **2002**, *41*, 2146.
- (42) Utracki, L. A. *Polymer Alloys and Blends*; Hanser Publishers: Munich, 1990.
- (43) Ishiaku, U. S.; Nasir, M.; Mohd Ishak, Z. A. *J. Vinyl Technol.* **1994**, *16*, 226.

MA0621066